scientific reports

Check for updates

OPEN

Electrochemical polymerized DL-phenylalanine modified carbon nanotube sensor for the selective and sensitive determination of caffeic acid with riboflavin

Kanthappa B[1], J. G. Manjunatha[1]✉, Sameh Mohamed Osman[2] & Narges Ataollahi[3]

In this study, DL-phenylalanine modified with a multiwall carbon nanotube paste electrode is used as advanced electrochemical sensor for analysing of 0.1 mM caffeic acid (CFA) with simultaneous detection of riboflavin (RFN). The developed sensors include electrochemically polymerized DL-phenylalanine (DL-PA) modified multiwall carbon nanotube paste electrode [DL-PAMMCNTPE] and bare multiwall carbon nanotube paste electrode [BMCNTPE]. The increasing stability in the developed electrochemical sensor for the quantification of CFA is highlighted in detail, along with its characterization using voltammetric techniques such as electrochemical impedance spectroscopy (EIS), cyclic voltammetry (CV), differential pulse voltammetry (DPV), and linear Sweep Voltammetry (LSV). Scanning electron microscopy (SEM) technique was used to studied the structural analysis of BMCNTPE and DL-PAMMCNTPE surface. The investigation of 0.1 mM CFA in 0.2 M phosphate buffered solution (PBS) using a 7.0 pH at 0.1 V/s scan rate was highlighted using DL-PAMMCNTPE, which shows good electrochemical responses compared to BMCNTPE. This work characterizes the voltammetric responses by inspecting the pH effect, scan rate effect, and concentration difference of CFA at the DL-PAMMCNTPE surface. The CFA responses specify that the scan rate progress is adsorption controlled. The concentration of CFA detection was started from 20 µM to 600 µM using DPV method, with lower limit of detection (LOD) of 0.280 µM and limit of quantification (LOQ) of 0.936 µM. And for CV method concentration range 20 to 550 µM, with LOD of 0.198 µM and LOQ of 0.702 µM. Furthermore, the developed electrochemical sensor responses are shows good stability, repeatability, and reproducibility, for CFA. The analytical applicability of CFA in apple juice and coffee powder samples was also evaluated.

Keywords Caffeic acid, DL-phenylalanine, Electrochemical analyser, Multiwall carbon nanotube paste sensor, Voltammetry

The growing concerns about antibiotic residues in various environments have encouraged the development of advanced sensing platforms for caffeic acid (CFA) detection. CFA is a naturally occurring organic compound belonging to the phenolic acid group and is widely distributed in plant-based food, particularly fruits (such as grapes, apples, and strawberries), vegetables (including kale flavour, cauliflower, and cabbage), and beverages like coffee. Chemically classified as hydroxycinnamic acid, CFA is recognized for its potential health-promoting effects[1,2]. Beyond its role as a flavor enhancer, recent studies have revealed its diverse living activities, with including the antioxidant, antibacterial, anti-cancer, anti-inflammatory, and immune-modulating properties. The antioxidant capacity of CFA is particularly noteworthy, playing a crucial role in neutralizing oxidative stress and mitigating cellular damage. The interaction between CFA and cellular processes, such as swelling and apoptosis, will be inspected to unravel the mechanisms of its therapeutic effects. The molecular structure of CFA exhibits two hydroxyl group around an aromatic ring, contributing to its distinctive antioxidant nature[3–6]. In the

[1]Department of Chemistry, FMKMC College, Constituent College of Mangalore University, Madikeri, Karnataka, India571201. [2]Chemistry Department, College of Science, King Saud University, P.O. Box 2455, 11451 Riyadh, Saudi Arabia. [3]Department of Civil, Environmental and Mechanical Engineering, University of Trento, Via Mesiano, 77, 38123 Trento, Italy. ✉email: manju1853@gmail.com

realm of wine, abundant CFA derivatives preserve colour and safeguard the alcoholic beverage from oxidative determination. Scientific studies suggest that CFA acts as an antitumor agent and may mitigate the effects of diabetes and cancer[7–12]. Various analytical technique has previously focused on quantitatively determining CFA, such as liquid chromatography[13,14], electrospray ionization mass spectrometry[15,16], capillary electrophoresis[17,18], capillary gas chromatographical method[19], and high-performance liquid chromatography[20–22]. Comparing these techniques to voltammetric methods, it becomes apparent that they are more time-consuming and require complex facilities, as well as highly qualified professionals to operate associated devices. Electroanalytical methods easily emerge as the most cost-effective, sensitive, and quick detection of CFA.

In this research, the electrochemical detection of CFA was using a DL-PAMMCNTPE. The usefulness of electrochemical approaches heavily relies on the choice of working electrode materials. Presently, carbon nanotubes (CNTs) are observed as the optimal material in the electrochemical sensor arena for bioactive compounds detection. This preference is attributed to various distinguishing characteristics, such as good conductivity, thermal stability, large electroactive surface area, superior mechanical, and outstanding biocompatibility, cost-effectiveness, upfront preparation methods, minimal background current during stable voltammograms[23–26]. The application of CNT material is crucial in the research field, and it presents positions CNTs as essential sensing tools in the current research for the more sensitivity and selectivity detection of CFA. The derivative of CNT materials shows the ability for application in oxygen reduction, exhibiting enhanced electrocatalytic activity, ionic strength, semi-ionic, and covalent banding, as well as outstanding chemical inertness[27–38]. In this work, the amino acid is a surface activator to increase the electrocatalytic action of the base conductor material. Electro-polymerized amino acid electrodes, particularly DL-PA, are first time used for the detection of CFA. DL-PA establishes increased sensitivity, biocompatibility, stability, and electrode surface features more active sites conducting networks[39], Finally, the electrochemically polymerized DL-PAMMCNTPE is a newly developed analytical application, and CFA was tested in various food and fruit juice samples.

Experimental

Instrumentation

Electrochemical analyses, including EIS, CV, and DPV method were studied using an electrochemical workstation (CHI-6038E) bought from the USA. The experimental arrangement involved an electrochemical cell equipped with three separate electrodes, a BMCNTPE and electrochemically polymerized DL-PAMMCNTPE is served as the working electrodes, a saturated calomel electrode (SCE) acted as the reference electrode, and a platinum wire functional as the auxiliary electrode. All researches were performed at the laboratory room temperature of 25 °C. The obtained data was stored in a computer connected to the electrochemical analyser. SEM pictures provided in the Vijnana Bhavan, Mysore University, Manasa Gangotri, India.

Reagents and chemicals

In this research work, various chemicals and reagents were used, including caffeic acid and multiwall carbon nanotube was supplied by the Tokyo chemical industry (Japan). DL-phenylalanine and silicon oil purchased from Molychem (India). Sodium phosphate monobasic monohydrate ($NaHPO_4.H_2O$), sodium phosphate dibasic dehydrate ($Na_2HPO_4.2H_2O$), and potassium ferrocyanide $K_4[Fe(CN)_6]$ were bought from Himedia (India). Potassium chloride (KCl) was purchased from Nice Chemicals in India. Each chemical was used at the laboratory temperature of 25 °C. A specific quantity of each substance was suspended in distilled water to make the essential chemical stock solution.

Preparation of real sample in coffee power

A small amount of coffee powder was weighed and then diluted with the organic solvent (ethanol). The mix was allotted to stand for one hour. After this period, the filter paper was used to filter the mixed sample, and the resulting solution was made adjusted to a total volume of 25 ml using distilled water. This solution is now referred to as the stock solution, and it is used to assess the analytical applicability of CFA.

Preparation of BMCNTPE

Carbon nanotubes and silicon oil (60:40%) were methodically combined and mixed in a mortar, grinding for five to ten minutes until a smooth paste was achieved. The resulting paste was tightly filled into a Teflon tube cavity with a 3 mm on the interior, and tissue paper was used to smooth out the surface, creating a uniform electrode's surface this is known as BMCNTPE. An electrical connection was established between the paste and a copper wire to enable the flow of electric power.

Results and discussions

Electro-polymerisation of DL-PA on BMCNTPE surface

To optimize the electro-activity of CFA, we trialled with changing the number of CV cycles conducted during the polymerization process before electrochemically polymerizing DL-PA on BMCNTPE. The CV cycles were optimized from 5 to 25. The highest current responses for CFA were observed at 10 CV cycles, including 5, 15, 20, and 25 CV cycles (Fig. 1b). Therefore, it was determined that 10 cycles were ideal for the electro-polymerization of DL-PA on the BMCNTPE through the research. Using the CV approach, DL-PA was electrochemically polymerized (10 cycles) on BMCNTPE in 0.2 M PBS, pH 7.0 at a 0.1 V/s scan rate. The corresponding plot is presented in Fig. 1a, it was observed that the peak current improved as the electrochemically polymerized sweep potential from -1.0 to 2.0 V, and the CV cycle inclined towards positive potential. This illustrates the conversion of DL-PA monomers into an electro-polymerization layer at the surface of electrode. Following the

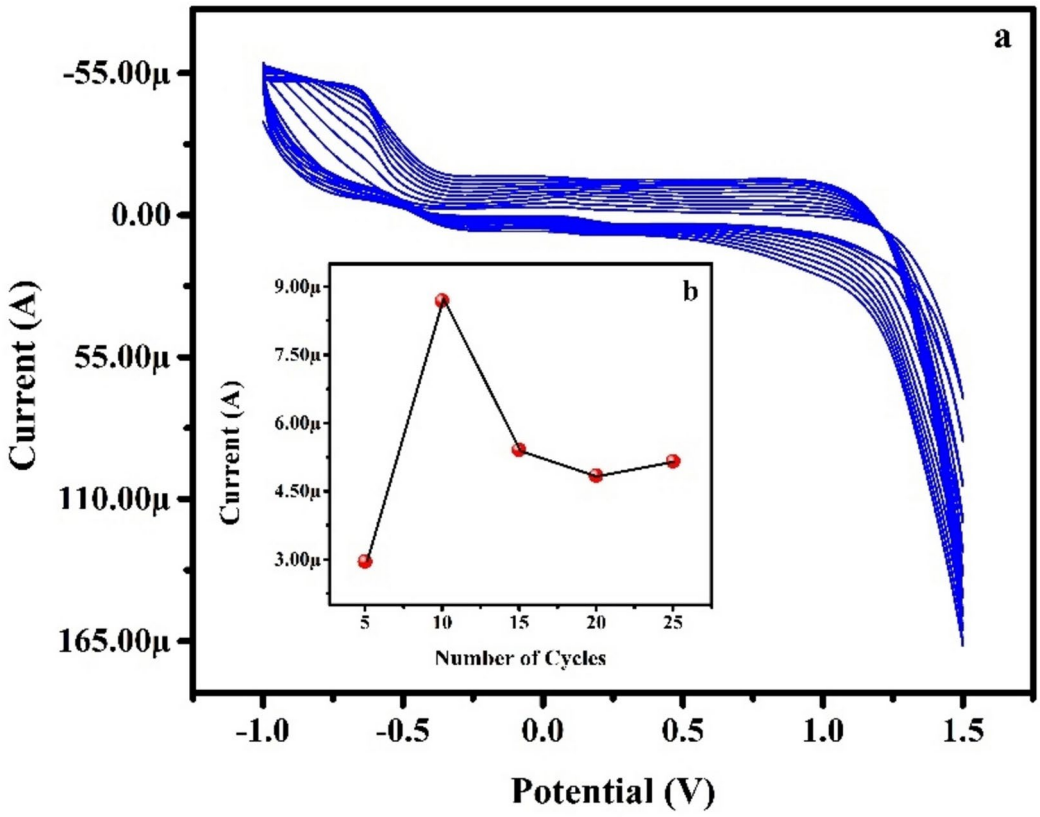

Fig. 1. (**a**) 10 Cyclic voltammograms (CVs) of polymerized DL-PA at the surface of BMCNTPE in PBS pH 7.0. at the scan rate of 0.1 V/s. Graph (**b**) plotted number of cycles vs current.

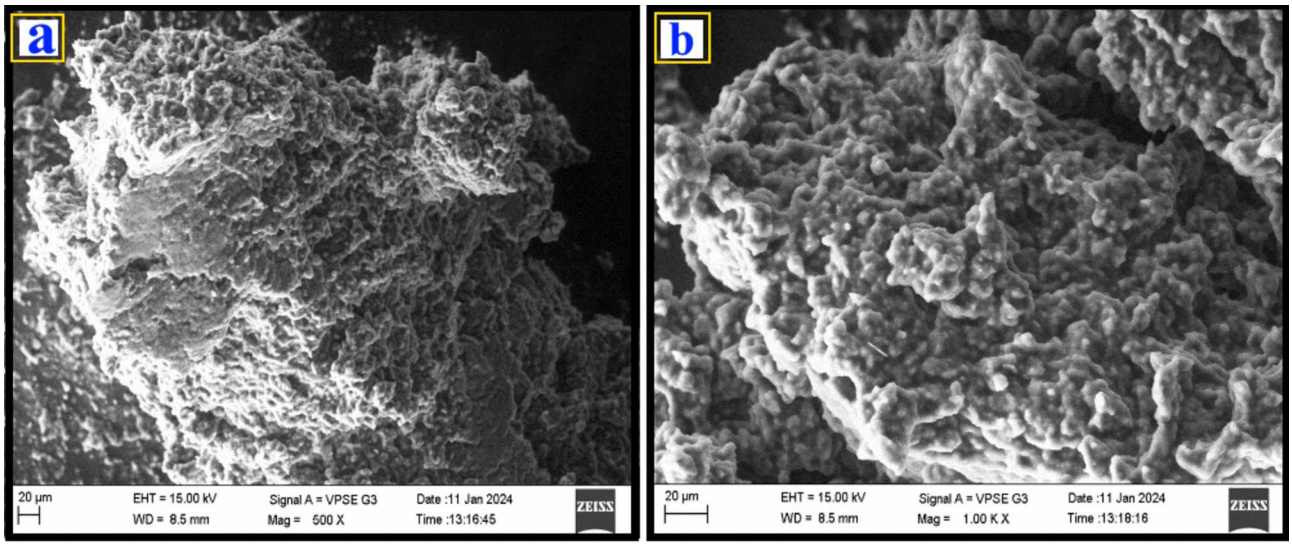

Fig. 2. SEM pictures of (**a**) BMCNTPE (**b**) DL-PAMMCNTPE.

electro-polymerization process, the resulting electrode was rinsed using distilled water before being utilized in successive experiments.

Structural analysis of SEM

The morphological structures of BMCNTPE and electrochemically polymerized DL-PAMMCNTPE were characterized using SEM technique, and an assessment is presented in Fig. 2. Figure 2a represents the BMCNTPE surface in absences of DL-PA, and it shows a random distribution of carbon nanotube layers. In Fig. 2b the DL-

PAMMCNTPE surface, DL-PA is evenly distributed in a layered fashion, displaying a symmetrical and tube-like structure was observed.

The study of EIS

In this study, we investigated the charge transfer resistance (Rct) and conductance of the developed electrode materials were examined using EIS. The EIS analysis of both BMCNTPE and DL-PAMMCNTPE, developed through an electrochemical polymerization process, was performed using a supporting electrolyte containing 1.0 mM $K_4[Fe(CN)_6]$ in 0.1 M KCl. Figure 3 presents the Nyquist plots for BMCNTPE (curve-b) and DL-PAMMCNTPE (curve-a). In this case, the BMCNTPE exhibits a larger semicircle representing less electrochemical active sites and lower electron conductivity. In difference, DL-PAMMCNTPE shows a smaller semicircle, signifying higher electron conductivity and lower charge transfer resistance due to the presence of more electroactive sites. The reduced semicircle size of DL-PAMMCNTPE demonstrations it superior conductivity and lower Rct comparison to BMCNTPE.

Study of electrochemical active surface area

The electro-activity and active surface area of DL-PAMMCNTPE (cycle-a) and BMCNTPE (cycle-b) were studied using the CV methods with a redox response in1.0 mM $K_4[Fe(CN)_6]$ in 0.1 M KCl as shown in Fig. 4. In this case, the DL-PAMMCNTPE outperforms of BMCNTPE surface terms of electrochemical activity indicated by greater redox peak current. This data highlights the significance of the DL-PA electrochemically polymerized layer on BMCNTPE. The improved electro-activity can be qualified to an increased surface-active area and a greater number of active sites on the electrode materials. The active surface area of BMCNTPE and DL-PAMMCNTPE were determined using the Randles–sevcik equation[40,41].

$$\mathrm{Ip} = 2.69 \times 10^5 \mathrm{n}^{3/2} \mathrm{A}\ \mathrm{D}^{1/2} \upsilon^{1/2} \mathrm{C} \tag{1}$$

In the randles–sevcik equation, "Ip" stands for peak current of bare and modified electrode, "n" reparents the electron numbers involved in the redox reaction of $K_4[Fe(CN)_6]$, "A" denotes the active surface area electrodes (cm^2), "D" stands for the diffusion coefficient (cm^2 /s), "C" signifies the $K_4[Fe(CN)_6]$ concentration (mM), and "υ" represents the scan rate (V/s). DL-PAMMCNTPE and BMCNTPE have calculated electroactive surface area of 0.0213 cm^2 and 0.0072 cm^2, respectively.

Impact of pH

In this study, impact of pH is a primary focus, constituting a main experiment in our study. Using the CV method, we discovered the effect of the pH solution on electrochemical responses of 0.1 mM CFA at the surface of DL-PAMMCNTPE. The investigation involved varying the pH from 5.5 to 7.5 at a scan rate of 0.1 V/s. Figure 5a shows an increase in pH peak current from 5.5 to 7.0 followed by decreases. In Fig. 5b, the plot of I_{pa} vs pH shows

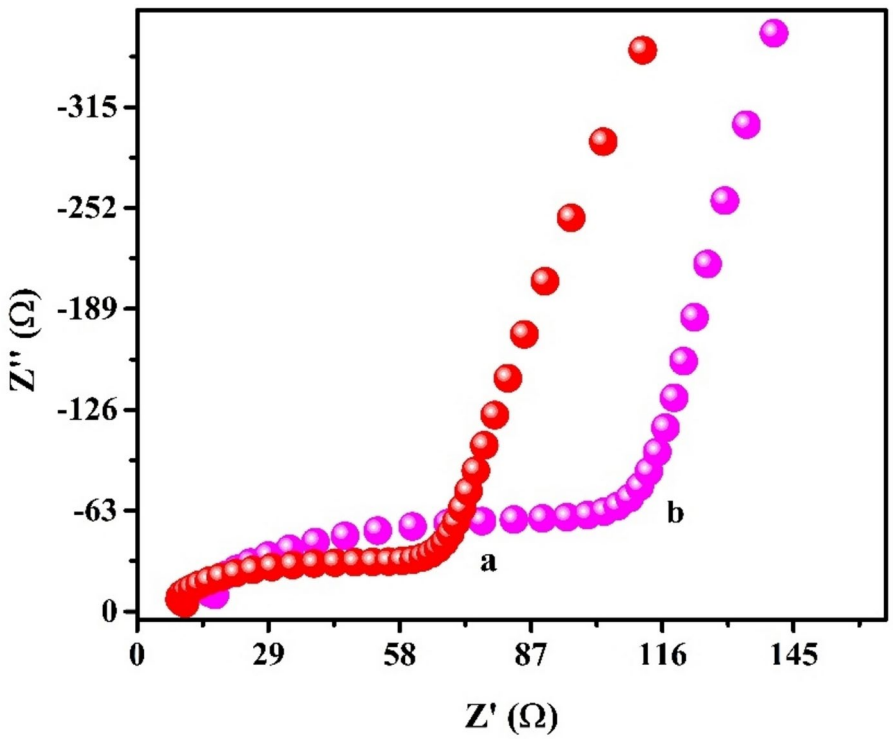

Fig. 3. EIS curves of (**a**) DL-PAMMCNTPE and (**b**) BMCNTPE.

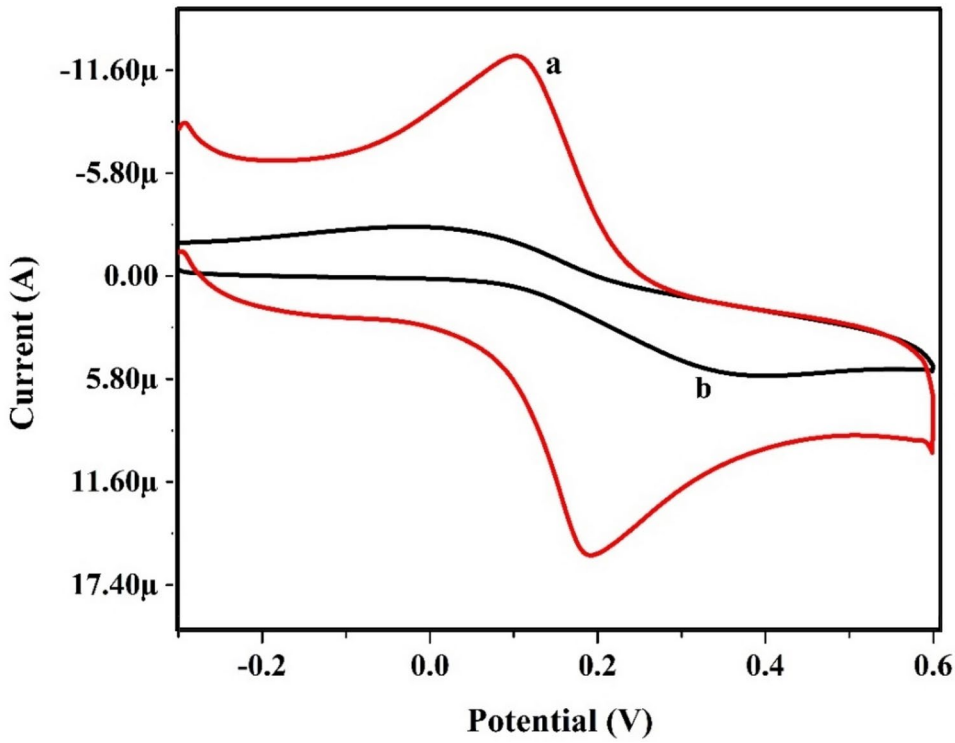

Fig. 4. CVs of 1.0 mM $K_4[Fe(CN)_6]$ in 0.1 M KCl on DL-PAMMCNTPE (cycle-a) and BMCNTPE (cycle-b) surface at the scan rate 0.1 V/s.

a shift of the electrochemical oxidation peak potential towards the positive direction as the pH varied from 5.5 to 7.5, with the peak current reaching its maximum at pH 7.0. Figure 5c presents the plot of E_{pa} vs pH, indicating an increase in peak current and a decrease in peak potential. The plot shows good linearity, with the corresponding relative equation being $E_{pa} = 0.558 - 0.061$ (V/pH) ($R^2 = 0.997$). Since the slope value in this case (-0.061 V/pH) is close to the theoretical value of – 0.059 V/pH, it suggests that the same number of protons and electrons are involved in the redox reaction of CFA. The number of protons was determined using the following equation.

$$m = \frac{B \times n \times F}{-2.303 \times R \times T} \tag{2}$$

The number of protons was found to be 2.07, which is close to 2 protons. This indicates enhanced electrostatic contact between the electrode surface and CFA, simplifying faster electron transfer. Based on our results, we selected that a pH 7.0 is optimal for this study, and we used this pH for all parameter studies.

Consequence of scan rate on DL-PAMMCNTPE surface

The CV method was utilized to assess the impact of the scan rate on the electrochemical response of 0.1 mM CFA in 0.2 M PBS at pH 7.0 on a DL-PAMMCNTPE surface. Scan rates varied from 0.025 V/s to 0.450 V/s, with a potential gap ranged from -0.4 to0.6 V. Figure 6a demonstrates that the scan rate impacts both peak potential and current. As the scan rate increases, the redox peak current rises, while the anodic peak potential shifts to the right side and the cathodic peak potential to the left side direction. The correlation between the plots of log υ vs log I_{pa} and I_{pc} (Fig. 6b) and υ vs I_{pa} and I_{pc} (Fig. 6c) is presented as follows: log ($I_{pa,}$ A) = —4.219 + 0.947 log (υ, A/V/s) ($R^2 = 0.998$), log ($I_{pc,}$ A) = 4.248(-0.977) log (υ, A/V/s) ($R^2 = 0.999$), υ vs I_{pa} (A) = $1.570 + 5.784 \times 10^{-5}$ υ (A/V/s) ($R^2 = 0.999$) I_{pc} (A) = $3.747 + 6.379 \times 10^{-5}$ υ (A/V/s) ($R^2 = 0.999$) are the corresponding relationships. The linear regression coefficient ($R^2 = 0.998$) and slope (0.947 A/V/s) of the log υ vs log I_{pa} and υ vs I_p plot are close to the theoretic value of 1, indicating that the process of CFA on the surface of DL-PAMMCNTPE primarily follows an adsorption-controlled pathway. This relationship is employed to determine the number of electrons participating in the CFA redox reaction constructed on Laviron's relative, Fig. 6d shows a well-associated linear correlation between log υ vs E_{pa} and E_{pc} expressed as follows: $E_{pa,}$ V = 0.164 + 0.051 log (υ, A/V/s) ($R^2 = 0.998$), E_{pc}, V = 0.024–0.0215 log (υ, A/V/s) ($R^2 = 0.993$).

$$B = \frac{2.303RT}{(1-\alpha)\,nF} \tag{3}$$

$$B = \frac{2.303RT}{\propto nF} \tag{4}$$

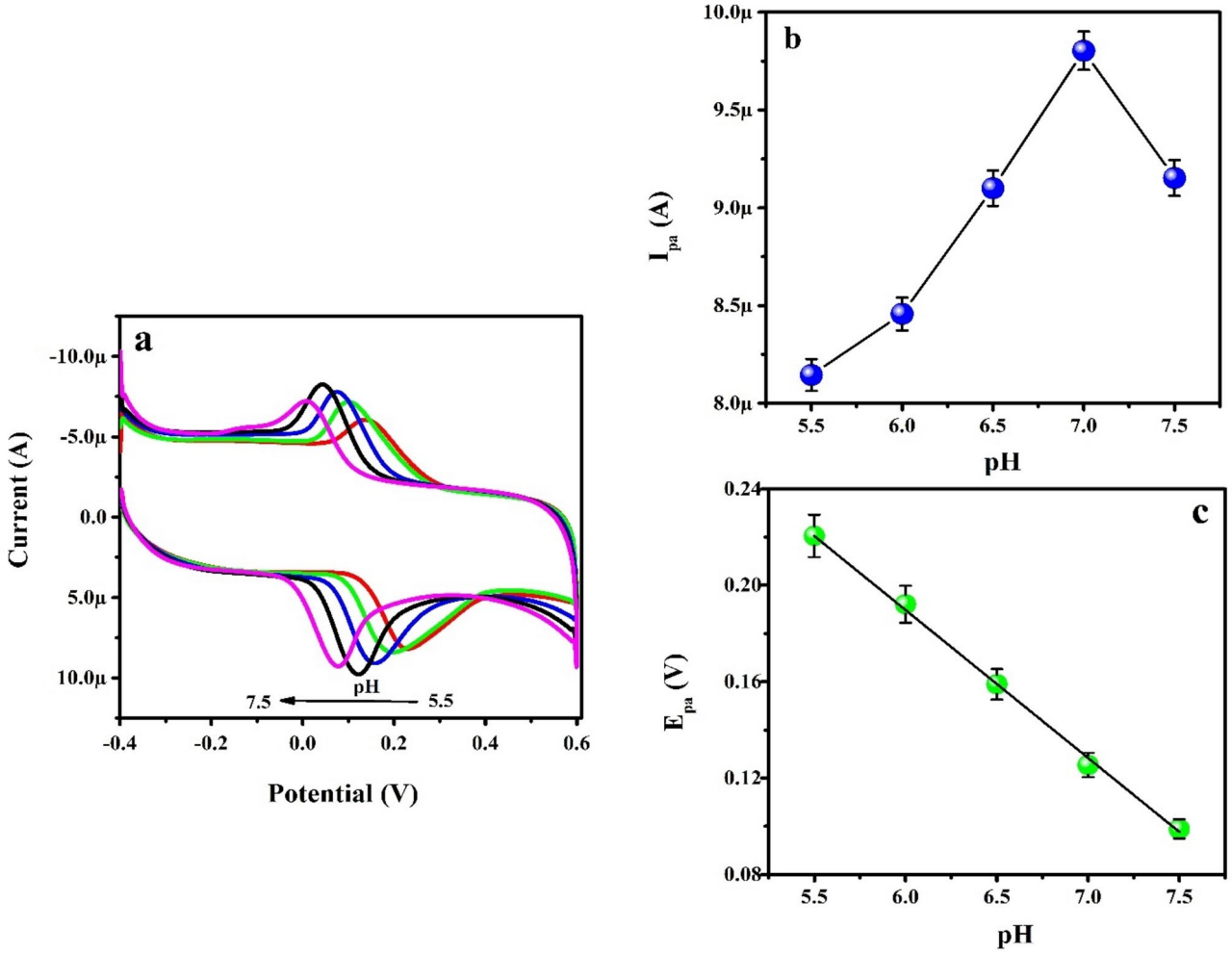

Fig. 5. (**a**) CVs of 0.1 mM CFA on DL-PAMMCNTPE surface in 0.2 M PBS with different pH from 5.5 to 7.5. at 0.1 V/s scan rate. Plot of (**b**) I_{pa} vs pH and (**c**) E_{pa} vs pH.

In this context, B is expressed as the slope of the plot log υ vs E_{pa}, number of electrons involved in the redox reaction of CFA is denoted by n, the charge transfer co efficient is represented as α, Faraday's constant is expressed as F, T represents the temperature and R represents universal gas constant. The number of transferred electrons involved in the CFA redox reaction at the DL-PAMMCNTPE surface has been calculated to be 1.88, approximately 2 electrons. And probable electrochemical reaction was shown in Fig. 7. Furthermore, using the following relation, the coverage concentration surface (Γ) of CFA on electrochemically polymerized DL-PAMMCNTPE was calculated.

$$\Gamma = \frac{\emptyset}{nFA} \tag{5}$$

The surface coverage Of CFA on DL-PAMMCNTPE was estimated and resolute designate 4.328 A^0 M/cm^2.

Electrochemical performance of CFA on BMCNTPE and DL-PAMMCNTPE surface

The electrochemical performance was analysed using the CV technique with a 0.1 V/s scan rate and a probable potential gap from -0.4 to 0.6 V. We examined the electrochemical redox responses of CFA on the BMCNTPE (cycle-a) and DL-PAMMCNTPE (cycle-c) surface, along with the presence and nonappearance (referred to blank, where lone PBS of 0.2 M with pH 7.0 is present cycle-b) as revealed in Fig. 8. In this investigation, the modified electrode surface of DL-PAMMCNTPE exhibited greater redox peak responses of CFA with a lower peak potential than the BMCNTPE. This enhancement results from the modification of the DL-PA polymer film, which increases the electrochemical active surface area of CFA, as well as the electrostatics connection between materials and active sites. Furthermore, in the nonappearance of CFA, there was no electrochemical activity on the surface of DL-PAMMCNTPE. This study reveals for the presence of CFA at the electrochemically polymerized DL-PAMMCNTPE surface enhances the electrochemical activity.

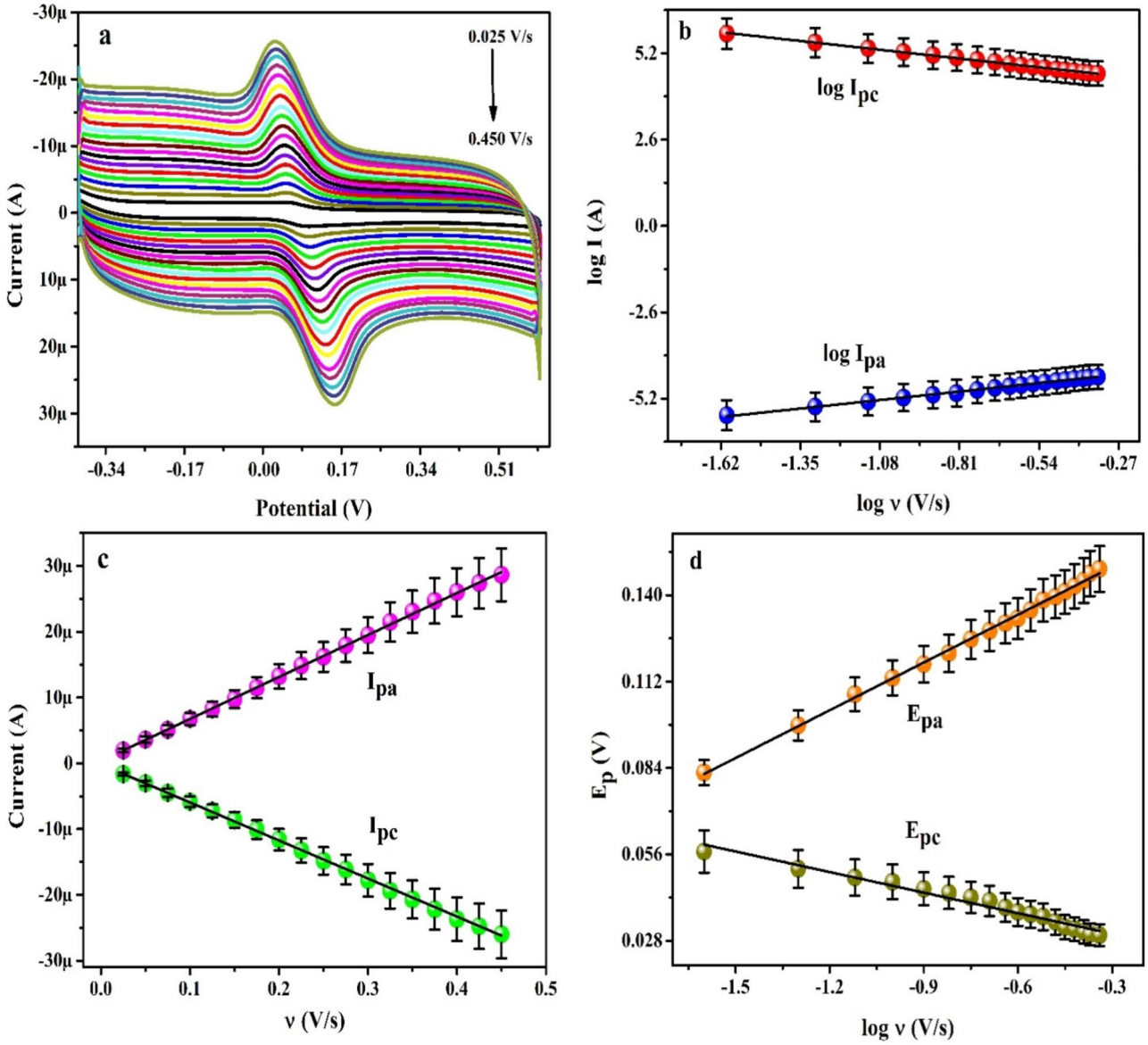

Fig. 6. (**a**) The CVs of 0.1 mM CFA on the surface of DL-PAMMCNTPE in PBS pH 7.0 at changed scan rate from 0.025 to 0.450 V/s ranges. Plot of (**b**) log υ vs log I, (**c**) υ vs Current, and (d) log υ vs Ep.

Concentration variation of CFA at DL-PAMMCNTPE surface

The concentration variation of CFA was analysed using the DPV and CV method. The CFA concentration was varied in systematically from 20 to 600 µM on the DL-PAMMCNTPE surface in PBS with a pH of 7.0, at 0.1 V/s scan rate using DPV method. Figure 9a, presents a plot of potential versus current, the CFA concentration was changes from 20 to 600 µM as the concentration of CFA increases, its peak current also increases, it exhibiting a good linearity. In Fig. 9b, a graph was plotted based on the observed data to represent the association amongst I_{pa} vs concentration of CFA peak current. The graph exhibits a strong linear correlation over the concentration ranged of 0.2 to 6.0 mM. The corresponding relationship is expressed as I_{pa} (A) = $1.2028 \times 10^{-5} + 0.3603$ [CFA] (A/[CFA]) with an ($R^2 = 0.998$). By using the calibration plot slope (0.3603) and the five blank CV curves successive of standard deviation (SD), the LOD and LOQ for CFA on the DL-PAMMCNTPE surface were determined by using the relations LOD = 3SD/B and LOQ = 10SD/B. Correspondingly, wherever B denotes slope of the I_{pa} vs concentration of CFA diagram 8b and S represented by SD of blank. The estimated values for LOD are 0.280 µM and LOQ 0.936 µM respectively. Figure 10a shows that the concertation variation of CFA using CV method ranges from 20 µM to 550 µM at the scan rate of 0.1 V/s. In Fig. 10b, a graph was plotted amongst Ipa vs concentration of CFA it shows good linear correlation. The corresponding relationship is expressed as Ipa (A) = $1.1284 \times 10^{-5} + 0.0471$ [CFA] (A/[CFA]) with an ($R^2 = 0.997$). The estimated LOD values is 0.198 µM and LOQ for 0.702 µM similarly. Table 1 provides a comparison of LOD value with pervious

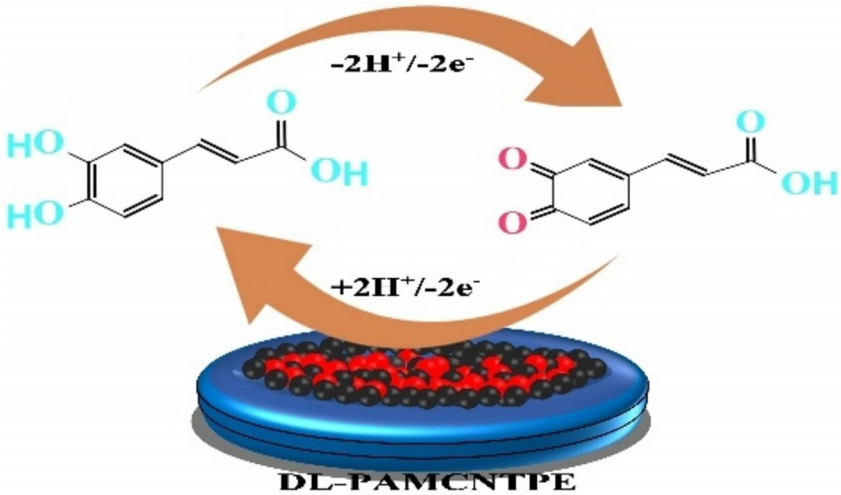

Fig. 7. Electrochemical redox reaction of CFA.

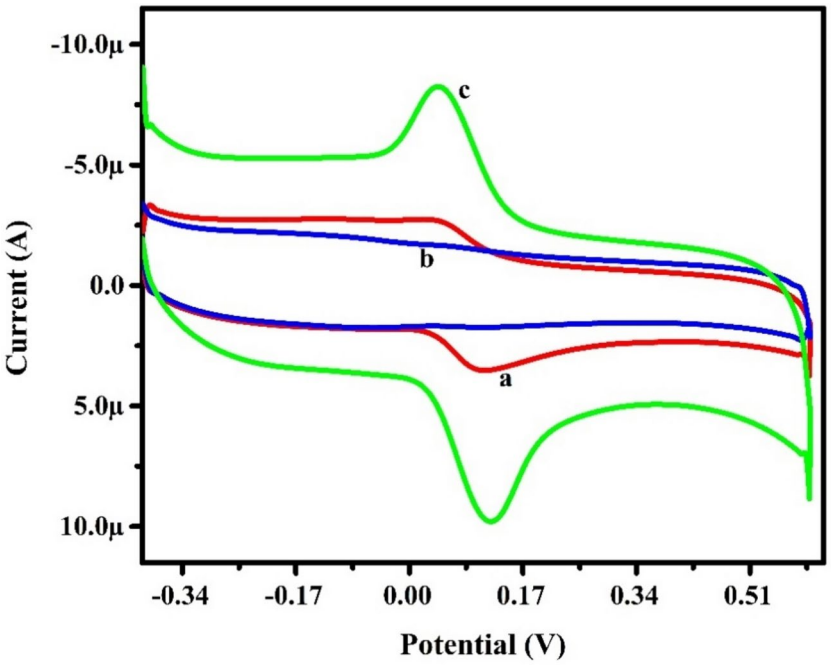

Fig. 8. CVs of 0.1 mM CFA for the presence and absence in PBS of pH 7.0 on the surface BMCNTPE (cycle-**a**) DL-PAMMCNTPE (cycle-**c**) and (blank, cycle-**b**) at 0.1 V/s scan rate.

publications[42,43,44,45,46,47,48,49]. The results assessment determines that the developed CFA sensor and the employed technique offer a suitable LOD for the detection of CFA.

Interference analysis on DL-PAMMCNTPE

The selectivity of the probable electrode for the detection of CFA was evaluated amidst various metal ions and organic molecules within a 0.2 M PBS at pH 7.0, using 0.1 V/s scan rate. The resulting is illustrated in Fig. 11. The 0.1 mM CFA detection was carried out in the appearance of metal ions such as Mg^{2+}, K+, Cu^{2+}, Zn^{2}+, Fe^{2+} Ca^{2+}, and 1.0 mM organic molecules like, valine (VLN), folic acid (FA), uric acid (UA), rutine (RT), and dopamine (DA). The impact of these molecules on the redox behavior of CFA was found to be insignificantly low. The relative error for CFA estimation in the presence of these interferents was maintained below ± 5%, this indicating that the prepared electrode exhibits excellent selectivity and is free from interference.

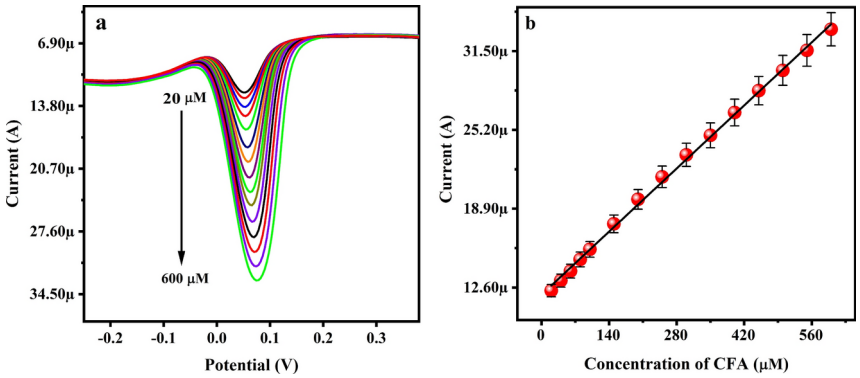

Fig. 9. (**a**) Differential pulse voltammograms were recorded for CFA across a concentration range spanning from 20 to 600 µM. these measurements were carried out in 0.2 M PBS at a pH of 7.0, at 0.1 V/s scan rate. Plot of (**b**) concentration of CFA vs current.

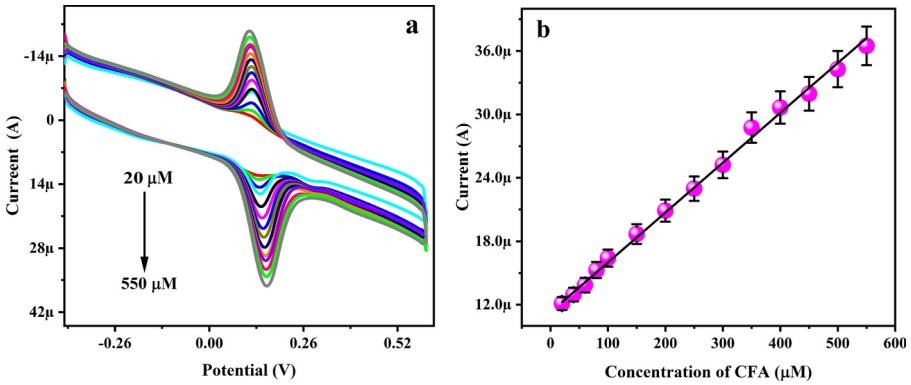

Fig. 10. (**a**) CVs recorded for CFA concentration range 20 to 550 µM in 0.2 M PBS a pH 7.0, at scan rate of 0.1 V/s. Plot of (**b**) current vs concentration of CFA.

Modified electrodes	Methods	Linear range (µM)	LOD (µM)	Reference
Molecularly-imprinted siloxanes	DPV	0.500–60.0	0.15	[42]
Glassy polymeric carbon	DPV	0.1–96.5	0.29	[43]
PtNi/C/GCE	DPV	0.75–591.783	0.5	[44]
Laccase-MWCNT-chitosan/Au	Amperometric	0.7–10	0.15	[45]
Poly (Glutamic acid)/GCE	CV	4.0–30.0	3.91	[46]
MnO_2/CM/GCE	SWV	1.00–15.00	0.27	[47]
Au@α-Fe2O3f.@RGO@GCE	DPV	19–1869	0.95	[48]
PtAuRu/GCE	DPV	-	0.39	[49]
	DPV	20–600	0.28	
DL-PAMMCNTPE	CV	20–550	0.19	Present work

Table 1. Comparison were made between the LOD values and methodologies of various previously published sensors.

Simultaneous study of CFA with RFN at BMCNTPE and DL-PAMMCNTPE surface

In simultaneous analysis CV and DPV methods shows the presence of CFA and RFN on surface of BMCNTPE (curve-a) and DL-PAMMCNTPE (curev-b). A solution containing 0.1 mM CFA was examined in the presence of 0.1 mM RFN, employing a scan rate of 0.1 V/s in a 0.2 M PBS solution at a pH of 6.0. In Fig. 12a and b, BMCNTPE (curve-a) shows lesser electrochemical activities, as demonstrated by a reduction in the oxidation peak current for both CFA and RFN as compared to DL-PAMMCNTPE (curve-b) show higher electrochemical activities in the redox reaction involving CFA with RFN peak current responses, and insignificant modification observed their absence or presence.

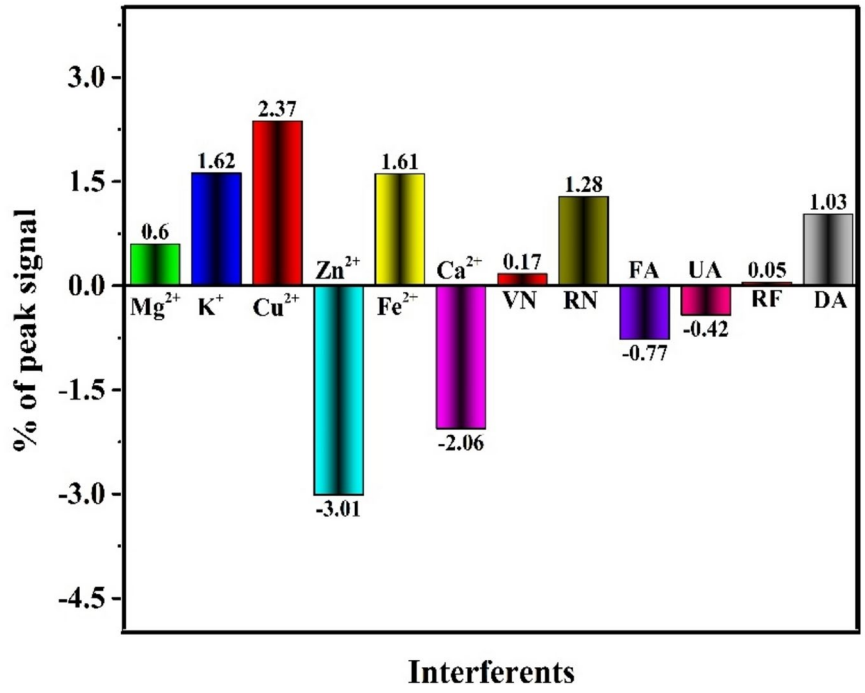

Fig. 11. Graph of % of peak signal vs interferents.

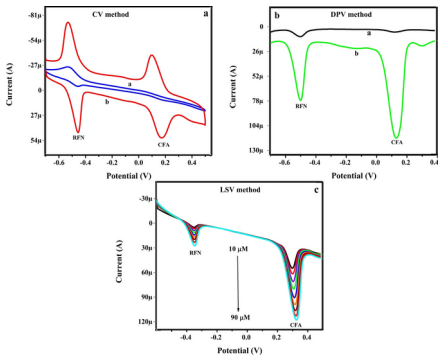

Fig. 12. Simultaneous analysis of CFA and RFN at BMCNTPE and DL-PAMMCNTPE (6.0 pH, 0.2 M PBS) at the scan rate of 0.1 V/s, using (**a**) CV method. (**b**) DPV method. (**c**) concentration variation of CFA and RFN ranges from 10 µM to 90 µM at DL-PAMMCNTPE surface using LSV method.

The simultaneously variation of CFA and RFN concentration was examined, using the LSV technique on the DL-PAMMCNTPE surface. In Fig. 12c, the plot represents the relationship between potential and current as the concentration of CFA and RFN varies from 10 µM to 90 µM in 0.2 M PBS at pH 7.0 with a scan rate of 0.1 V/s. Particularly, with increasing both CFA and RFN concentration its peak potential slightly shifting to negative direction, there's a corresponding raise in its peak current. This observation underscores the efficacy of modified sensor in detecting CFA and RFN among interfering substances, given that CFA and RFN does not influence other molecules. The CFA and RFN analyte exhibit stability in both peak current and potential signals, confirming the reliability of the detection mechanism.

Repeatability, Reproducibility, and Stability on DL-PAMMCNTPE

The potential electrochemically developed DL-PAMMCNTPE experienced a complete assessment of its repeatability, reproducibility, and stability using the CV method for the redox responses of CFA in a 0.2 M PBS with pH 7.0 at 0.1 V/s scan rate. Reproducibility stood assessed through 5 consecutive CV curves, where the electrode was renewed after each cycle while keeping CFA as the constant analyte at the surface of DL-PAMMCNTPE. The resulting relative standard deviation was determined to be approximately 1.025%, indicating excellent reproducibility. Repeatability was examined by conducting 5 consecutive CV curves for CFA, with the changing of analyte of each cycle end while maintaining the DL- PAMMCNTPE constant. The calculated relative standard deviation for test was approximately 0.544%, indicating the electrodes shows good repeatability. The

Real sample	Trail number	Added in (μM)	Found in (μM)	Recovery (%)
	1	0.2	0.192	96.4
Apple juice	2	0.4	0.389	97.4
	3	0.6	0.589	98.2
	4	0.8	0.776	97.0
	5	1.0	0.968	96.8
	1	0.2	0.196	98.0
Coffee powder	2	0.4	0.391	97.7
	3	0.6	0.568	94.6
	4	0.8	0.785	98.1
	5	1.0	0.986	98.6

Table 2. Recover percentage of CFA in caffeic acid containing sample.

stability of DL-PAMMCNTPE was studied by recording CV methods for CFA under optimized conditions after the electrode had been kept for 2 days in a locked container on area temperature (25°C). Upon successive detection of CFA from this electrode, it was observed only 3.71% of the CFA cycle current had degenerated associated toward the initial cycle current, confirming the excellent constancy of developed sensors.

Real sample analysis at DL-PAMMCNTPE surface

The selectivity of proposed electrochemically polymerized DL- PAMMCNTPE for the analysis of CFA in apple juice and coffee powder sample was explored using a DPV method. The analysis of CFA in apple juice samples demonstrated favourable recovery suing DL-PAMMCNTPE, ranging from 96.4% to 98.2%. The proposed methods proved effective assessed analytes in coffee powder stock solution, reaching a good recovery rate ranging from 94.6% to 98.6. The corresponding significances are presented in Table 2.

Conclusion

In this research, we efficiently prepared cost-effective and environmentally responsive electrochemical sensor, DL-PAMMCNTPE, and BMCNTPE using a straightforward procedure for the sensitive and selective analysis of CFA. The activation of the BMCNTPE surface involved the formation of an active DL-PA film through a simple electrochemically polymerization method. The resulting DL- PAMMCNTPE exhibited an increased electrochemical surface area, leading to a quicker transfer of electron rate frequency through CFA redox response and enhanced electrochemical activity. Surface characteristics of both DL-PAMMCNTPE and BMCNTPE were successfully characterized using SEM, and CV, DPV, and EIS methods shows good electrochemical responses for the CFA molecule. DL- PAMMCNTPE shows improved electrochemical response, showcasing a strong linear correlation, LOD, LOQ, and respectable repeatability, reproducibility, and good stability for analysing of CFA redox nature. Additionally, the electrochemically polymerized DL-PAMMCNTPE and DPV methods showed remarkable CFA recovery in fruit juice samples, ranging from 96.4% to 98.2%. and Coffee powder shows good recovery rate ranging from 94.6% to 98.6%.

Data availability

The datasets used and/or analysed during the current study available from the corresponding author on reasonable request.

Received: 13 October 2024; Accepted: 2 December 2024
Published online: 28 December 2024

References

1. Xu, X. et al. Carbon dots coated with molecularly imprinted polymers: A facile bioprobe for fluorescent determination of caffeic acid. *J. Colloid Interface Sci.* **529**, 568–574 (2018).
2. Li, J. et al. Facile synthesis of MnO2-embedded flower-like hierarchical porous carbon microspheres as an enhanced electrocatalyst for sensitive detection of caffeic acid. *Anal. Chim. Acta.* **985**, 155–165 (2017).
3. García-Guzmán, J. J. et al. Assessment of the polyphenol indices and antioxidant capacity for beers and wines using a tyrosinase-based biosensor prepared by sinusoidal current method. *Sensors* **19**, 66 (2018).
4. Bo, Z. et al. green preparation of reduced graphene oxide for sensing and energy storage applications. *Sci. Rep.* **4**, 4684 (2014).
5. Ramki, S. et al. Voltammetric determination of caffeic acid using Co3O4 microballs modified screen-printed carbon electrode. *Int. J. Electrochem. Sci.* **13**, 1241–1249 (2018).
6. Moreira, G. C. & de-Souza Dias, F. Mixture design and Doehlert matrix for optimization of the ultrasonic assisted extraction of caffeic acid, rutin, catechin and trans-cinnamic acid in Physalis angulata L. and determination by HPLC DAD. *Microchem.* J. **141**, 247–252 (2018).
7. Robards, K. & Antolovich, M. Analytical chemistry of fruit bioflavonoids A Review. *Analyst.* **122**, 11–34 (1997).
8. Hsu, F. L., Chen, Y. C. & Cheng, J. T. Caffeic acid as active principle from the fruit of xanthiumstrumarium to lower plasma glucose in diabetic rats. *Planta Med.* **66**, 228–230 (2000).
9. Nardini, M. et al. In vitro inhibition of the activity of phosphorylase kinase, protein kinase C and protein kinase A by caffeic acid and a procyanidin-rich pine bark (Pinus marittima) extract. *Biochim. Biophys. Acta (BBA) Gen. Subj.* **1474**, 219–225 (2000).
10. Alanko, J. et al. Modulation of arachidonic acid metabolism by phenols: Relation to their structure and antioxidant/prooxidant properties. *Free Radic. Biol. Med.* **26**, 193–201 (1999).

11. Kang, N. J. Caffeic acid a phenolic phytochemical in coffee, directly inhibits fyn kinase activity and UVB-induced COX-2 expression. *Carcinogenesis.* **30**, 321–330 (2009).
12. Robbins, R. J. Robbins, Phenolic acids in foods: An overview of analytical methodology. *J. Agric. Food Chem.* **51**, 2866–2887 (2003).
13. Urakova, I. N. et al. Development and validation of an LC method for simultaneous determination of ascorbic acid and three phenolic acids in sustained release tablets at single wavelength. *Chromatographia.* **67**, 709–713 (2008).
14. Cao, W. et al. LC with electrochemical detection for analysis of caffeic acid and caffeic acid phenyl ester in propolis. *Chromatographia.* **73**, 411–414 (2011).
15. Del Boccio, P. & Rotilio, D. Quantitative analysis of caffeic acid phenethyl ester in crude propolis by liquid chromatography-electrospray ionization mass spectrometry. *J. Separ. Sci.* **27**, 619–623 (2004).
16. Cech, N. B. et al. High-performance liquid chromatography/electrospray ionization mass spectrometry for simultaneous analysis of alkamides and caffeic acid derivatives from Echinacea purpurea extracts. *J. Chromatogr. A.* **1103**, 219–228 (2006).
17. Mancek, B. & Kreft, S. Determination of cichoric acid content in dried press juice of purple coneflower (Echinacea purpurea) with capillary electrophoresis. *Talanta.* **66**, 1094–1097 (2005).
18. Youyuan, P.; Fanghua, L. & Jiannong, Y. Determination of phenolic acids and flavones in lonicera japonica thumb. by capillary electrophoresis with electrochemical detection, *Electroanal.* **17**, 356–362 (2005).
19. Bankova, V., Christov, G., Stoev, G. & Popov, S. Determination of phenolics from propolis by capillary gas chromatography. *J. Chromatogr.* **607**, 150–153 (1992).
20. Michailof, C., Manesiotis, P. & Panayiotou, C. Synthesis of caffeic acid and p-hydroxybenzoic acid molecularly imprinted polymers and their application for the selective extraction of polyphenols from olive mill waste waters. *J. Chromatogr. A.* **1182**, 25–33 (2008).
21. Y. Xing, et al. Caffeic acid product from the highly copper-tolerant plant Elsholtzia splendens post phytoremediation: its extraction, purification, and identification. *J. Zhejiang Univ. Sci. B: Biomed. Biotechnol.* **13**, 487–493 (2012).
22. Wijngaard, H. H., Roßle, C. & Brunton, N. A survey of Irish fruit and vegetable € waste and by-products as a source of polyphenolic antioxidants. *Food Chemistry.* **116**, 202–207 (2009).
23. Teradale, A. B. et al. Synergetic effects of a poly-tartrazine/CTAB modified carbon paste electrode sensor towards simultaneous and interference-free determination of benzenediol isomers. *React. Chem. Eng.* **8**, 3071–3081 (2023).
24. Ganesh, P. S. et al. Electrochemical sensing of anti-inflammatory drug mesalazine in pharmaceutical samples at polymerized-congo red modified carbon paste electrode. *Chemical Physics Letters.* **806**, 140043 (2022).
25. Kailash, S. C. et al. Simultaneous sensing of mesalazine and folic acid at poly (murexide) modified glassy carbon electrode surface. *Materials Chemistry and Physics.* **290**, 126538 (2022).
26. Ganesh, P. S. et al. Role of electron transfer between bare electrode and benzoguanamine to fabricate an electrochemical sensor for drugs: Theoretical and electrochemical approach. *Microchemical Journal.* **201**, 110731 (2024).
27. Pushpanjali, P. A. et al. Voltammetric analysis of antihistamine drug cetirizine and paracetamol at poly(L-Leucine) layered carbon nanotube paste electrode. *Surf. Interfaces.* **24**, 101154 (2021).
28. Mazloum-Ardakani, M. et al. Simultaneous determination of epinephrine and acetaminophen concentrations using a novel carbon paste electrode prepared with 2,2′-1,2 butanediylbis (nitroethylene)]-bis-hydroquinone and TiO2 nanoparticles. *Colloids Surf. B.* **76**, 82–87 (2010).
29. Manjunatha, J. G. et al. Sodium dodecyl sulfate modified carbon nanotubes paste electrode as a novel sensor for the simultaneous determination of dopamine, ascorbic acid, and uric acid. *Comptes Rendus Chimie.* **17**, 465–476 (2014).
30. Beitollahi, H., Karimi-Maleh, H. & Khabazzadeh, H. Nanomolar and selective determination of epinephrine in the presence of norepinephrine using carbon paste electrode modified with carbon nanotubes and novel 2-(4-oxo-3-phenyl-3, 4-dihydro-quinazolinyl)-N′-phenyl- hydrazine carbothioamide. *Analytical Chemistry.* **80**, 9848–9851 (2008).
31. Hareesha, N. et al. Electrochemical analysis of indigo carmine in food and water samples using a poly (glutamic acid) layered multi-walled carbon nano-tube paste electrode. *J. Electron. Mater.* **50**, 1230–1238 (2021).
32. Manjunatha, J. G., Deraman, M., Basri, N. H. & Talib, I. A. Fabrication of poly (Solid Red A) modified carbon nano tube paste electrode and its application for simultaneous determination of epinephrine, uric acid and ascorbic acid. *Arabian journal of chemistry.* **11**, 149–158 (2018).
33. Mazloum Ardakani, M. et al. Electrocatalytic oxidation and nanomolar determination of guanine at the surface of a molybdenum (VI) complex–TiO2 nanoparticle modified carbon paste electrode. *J. Electroanal. Chem.* **624**, 73–78 (2008).
34. Ganesh, P. S. et al. An experimental and theoretical approach to electrochemical sensing of environmentally hazardous dihydroxy benzene isomers at polysorbate modified carbon paste electrode. *Sci Rep.* **12**, 2149 (2022).
35. Enyioma, C.O, et al. Eno E. Ebenso. Electrochemical evaluation of Cd2+ and Hg2+ ions in water using ZnO/Cu2ONPs/PANI modified SPCE electrode, *Sensing and Bio-Sensing Research*. **35**, 100476 (2022).
36. Elugoke, Saheed Eluwale, et al. "Sensitive and selective neurotransmitter epinephrine detection at a carbon quantum dots/copper oxide nanocomposite." *Journal of Electroanalytical Chemistry.* **929,** 117120 (2023).
37. Saheed, E. E. et al. Common Transition Metal Oxide Nanomaterials in Electrochemical Sensors for the Diagnosis of Monoamine Neurotransmitter-Related Disorders. *Chem ElectroChem.* **11**, e202300578 (2024).
38. Ganesh, P. S. et al. Quantum chemical studies and electrochemical investigations of pyrogallol red modified carbon paste electrode fabrication for sensor application. *Microchemical Journal.* **167**, 106260 (2021).
39. Ma, X. & Chao, M. Electrocatalytic determination of maltol in food products by cyclic voltammetry with a poly(l-phenylalanine) modified electrode. *Anal. Methods.* **5**, 5823 (2013).
40. Manjunatha, J.G. et al. Enhanced Electrochemical Detection of Rutin Using Poly (Methyl Orange) Modified Carbon Paste Electrode as a Responsive Electrochemical Sensor. *Chemistry Africa*. 1–10. (2024).
41. Sharmila, B. M. et al. Determination of Formoterol Fumarate in Pharmaceutical Formulations by Voltammetric Technique using a Novel Methyl Orange Layered Sensor. *Sensing and Imaging.* **25**, 7 (2023).
42. Leite, F.R.; F. Santos, W.D. J. R. & L.T. Kubota, Selective determination of caffeic acid in wines with electrochemical sensor based on molecularly imprinted siloxanes. *Sens. Actuator B-Chem.***193**, 238–246 (2014).
43. Fernando, D. H. L., Nelson, R. S. & Paulino, O. H. Determination of caffeic acid in red wine by voltammetric method. *Electroanalysis.* **20**, 1252–1258 (2008).
44. Erk, N. Voltammetric behaviour and determination of moxifloxacin in pharmaceutical products and human plasma. *Anal. Bioanal. Chem.* **378**, 1351–1356 (2004).
45. Diaconu, M., Litescu, S. & Radu, G. Laccase–MWCNT–chitosan biosensor—A new tool for total polyphenolic content evaluation from in vitro cultivated plants. *Sens. Actuator B-Chem.* **145**, 800–806 (2010).
46. Santos, D. P. et al. Application of a glassy carbon electrode modified with Poly (glutamic acid) in caffeic acid determination. *Microchim. Acta.* **151**, 127–134 (2005).
47. Li, J. et al. Facile synthesis of MnO2-embedded flower-like hierarchical porous carbon microspheres as an enhanced electrocatalyst for sensitive detection of caffeic acid. *Anal Chim Acta.* **985**, 155–165 (2017).
48. Bharath, G. et al. Facile synthesis of au@α-Fe2O3@RGO ternary nanocomposites for enhanced electrochemical sensing of caffeic acid toward biomedical applications. *J Alloys compounds.* **750**, 819–827 (2018).
49. Shi, Y. et al. Visible light enhanced electrochemical detection of caffeic acid with waxberry-like PtAuRu nanoparticles modified GCE. *Sens, Actuators B Chemical.* **272**, 135–138 (2018).

Acknowledgements
1. Kanthappa B, gratefully acknowledges the financial support from the SC/ST Cell for the SC/ST Fellowship (No. MU/SCTRF/CR5/2019-20/SCT-1), Mangalore University. 2. Dr. J.G. Manjunatha gratefully acknowledges the financial support from the VGST, Bangalore under Research Project. No. VGST/KFIST L-2/2022-23/GRD-1020. 3. Sameh Mohamed Osman, was gratefully acknowledging the financial supported by the Researchers Supporting Project (RSP2025R405), King Saud University, Riyadh, Saudi Arabia.

Author contributions
Authorship contribution statement Kanthappa B: Conceptualization, Formal analysis, Methodology, Software, Data curation, Visualization, Writing-original draft, Writing-review and editing. J.G. Manjunatha: Conceptualization, supervision, Formal analysis, Methodology, Data curation, Visualization, Writing-review and editing. Sameh Mohamed Osman: Conceptualization, Formal analysis. Narges Ataollahi: Conceptualization, Formal analysis.

Declarations

Competing interests
The authors declare no competing interests.

Additional information
Correspondence and requests for materials should be addressed to J.G.M.

Reprints and permissions information is available at www.nature.com/reprints.

Publisher's note Springer Nature remains neutral with regard to jurisdictional claims in published maps and institutional affiliations.